

PACS 07.07.Hj, 42.55.Px, 73.40.Qv

Radiation dynamics of injection lasers with saturating absorber in resonator

I.S. Manak

Belarusian State University, 4, Nezavisimosti Ave., 220050 Minsk, Belarus

Abstract. The structure of a GaAlAs laser with saturating absorber in a resonator and a method of research of the light generation dynamics with the use of an optical stroboscopic oscilloscope OSO-1 which has a time resolution of ~ 30 ps are described. The dependence of the succession frequency of radiation peaks on the parameters of pumping current impulses and the direct bias current in injection heterolasers with saturating absorber in a resonator is determined.

Keywords: injection laser, heterostructure, radiation dynamics, peaks, bias, saturating absorber, photocurrent strobbing, optical stroboscopic oscilloscope.

Manuscript received 25.05.07; accepted for publication 07.02.08; published online 25.02.08.

1. Introduction

None of the quantum electronic devices can compete with injection lasers (IL) possessing the unique combination of such advantages as a high efficiency of the direct transformation of the electric current energy into the coherent radiation, high amplification coefficient, low sluggishness, considerable width of the generation wavelength, miniature size of constructions, etc. The essential feature of the IL optical model is a significant optical non-linearity of the semiconductor medium that may be stipulated by the strong effect of free carriers on the refraction index and by the effect of the radiation intensity on their concentration. Dynamic phenomena stipulated by this effect are referred to crucial ones in the non-linear optics of semiconductor lasers.

To solve many metrological problems, it is required the use of exploitation-comfortable supplies of optical impulses with extremely little length, quite high succession frequency, shape repeatability, and rigid association with a synchronizing signal. The radiator of such a type can be made on the basis of an injection semiconductor laser. Generation of extremely short impulses by IL is interesting for such applications as optical communication with high-speed data transmission, superfast data processing, ranging, creating of optical-electron beams, and spectroscopy with pico- and femtosecond time resolution. Nowadays, many research works study the IL radiation dynamics with the purpose

of determining their processing speed and making the optical switching devices on their basis.

This paper is devoted to the study of the complicated dynamics of radiation generation in injection lasers on a double heterostructure with saturating absorber in a resonator.

2. Subject of research

Diodes of the structure shown in Fig. 1 were made by the method of liquid phase epitaxy in GaAlAs solid solutions. They consist of the five-layer structure with a GaAs active layer of $0.5 \mu\text{m}$ in thickness, in which the impurity of a concentration of $5 \times 10^{17} \text{ cm}^{-3}$ was introduced. The active layer is between two $\text{Ga}_{1-x}\text{Al}_x\text{As}$ emitters. In one of them, the Te impurity of $(0.5-1) \times 10^{18} \text{ cm}^{-3}$ in concentration was doped, and in the other one – Ge impurity of $(1-5) \times 10^{18} \text{ cm}^{-3}$ in concentration. The emitters' thicknesses were $1.5-2.5$ and $2-2.5 \mu\text{m}$, respectively. The Al concentration in both emitters is equal to $\sim 30\%$ that provides the symmetric and quite effective waveguide for radiation generated in the active layer.

To get the area with saturating absorber, the deep implantation of oxygen ions into one of the heterolaser reflectors was used. Oxygen ions were accelerated to an energy of 18.7 MeV by a cyclotron in the Ioffe PTI of RAS that provided their penetration to the depth of $10 \mu\text{m}$ [1]. This depth was approximately 5% of the laser diode resonator length. The choice of such long lengths of the absorption area was determined by the conditions to get stable oscillations.

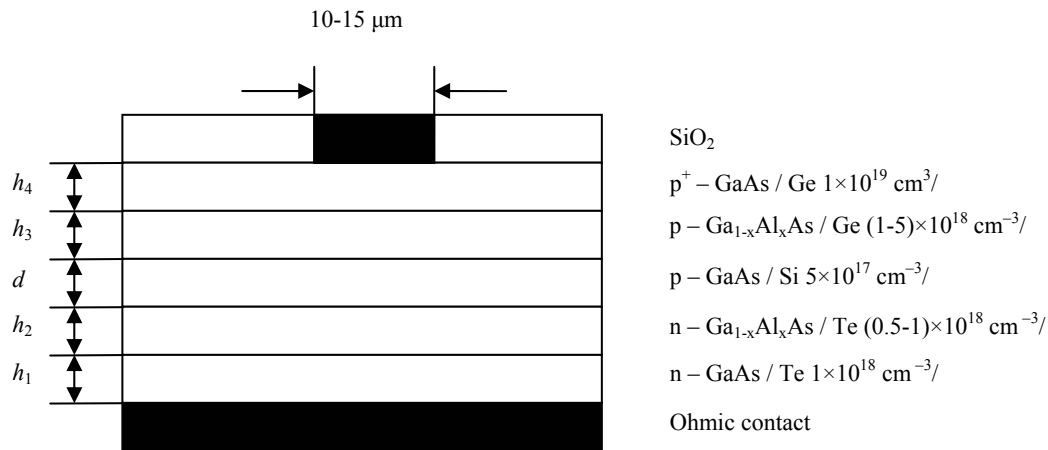


Fig. 1. Scheme of a stripline laser on a double heterostructure: $h_1=30-50 \mu\text{m}$, $h_2=1.5-2.5 \mu\text{m}$, $h_3=2-2.5 \mu\text{m}$, $h_4=2 \mu\text{m}$, $d=0.5 \mu\text{m}$.

3. Pumping of laser diodes

The pumping of injection heterolasers was made by an impulse generator with the formation of fronts on a diode with charge accumulation. The generator supplied impulses with a succession frequency of 50 kHz, lengths of 7, 8, and 10 ns, and leading edge lengths of 0.3, 2, and 4 ns, respectively, as well as impulses of 5 ns in length with leading edge lengths of 0.3, 2, and 4 ns and the amplitude up to 50 V at a 24-Ohm resistance.

4. Strobbing of the photocurrent in the near-cathode area of photomultipliers is the effective way to measure the parameters of short radiation impulses

The exploring of dynamic processes in semiconductor supplies of not very high power can be successfully done by single-quantum statistical photorecording methods [2], electro-optical chronography using electro-optical converters with beam time scanning [3], electrical heterodyning of the signal directly in a photoresistance [4], photodiode [5], and photoelectron multiplier (PEM) [6]. At studying the optical radiation modulated in the super high frequency (SHF) range, one can successfully use methods of frequency transformation or phase detection in a photoreceiver [7, 8]. In phase detectors with phase commutation to 180° , the time resolution of $\sim 2.5 \cdot 10^{-13}$ s is reached [9]. In the analysis of impulse optical signals in devices with electro-optical converters, one reaches the time resolution of $\sim 3 \cdot 10^{-13}$ s, but the dynamic range of linear registering of input signals is ~ 10 [10]. The use of the signal strobbing directly in a photodetector raises greatly the time resolution of the oscillography systems for optical signals as compared with the systems where photodetectors operate in the direct photorecording mode. For example, the possibility to create high-sensitivity photoregistering systems on PEMs for impulse optical signals with a time resolution of $3 \cdot 10^{-11}$ s was shown in [11]. But, all the more, the

general task of creation of compact devices for the express-registration of a form of optical signals of $10^{-7} - 10^{-3}$ W in power in the wavelength region of 0.4–1.3 μm with a time resolution of 10^{-11} s which are able to operate under optical noises and background radiation is always actual.

It is found out that the sluggishness of the processes of photoemission and secondary electron emission restricts the reachable time resolution of systems and devices in the measurement of the parameters of optical radiation by photoelectron multipliers. By taking the time dispersion of the electron output from a sensitive photolayer into account, one can speak about the limiting value of photocathode time resolution of 10^{-12} s [12]. This value can be decreased by decreasing the photolayer thickness, but the photocathode sensitivity will also decrease in this case. The time dispersion of second electron emission is estimated experimentally by the limit values of $10^{-14} - 10^{-12}$ s for metals and metal compounds and by $10^{-12} - 10^{-9}$ s for the most effective emitters on dielectrics, semiconductors, and their compounds [13]. The high-operation speed of photo- and secondary electron emissions from solid-body surfaces point out to the possibility to create photoelectron devices with a time resolution of 10^{-12} s. The sluggishness of photoelements with extrinsic photoeffect is determined by the time dispersion t_{fl} of the electron fly-pass from the photocathode to a plate. This time dispersion, in turn, depends on the speed and start angle of the electron output from the cathode, which results in the difference between their paths. The time t_{fl} determines not only the time of generation of the photocurrent in a plate load but also the leading edge of photoelement impulses, i.e. the response characteristic. The decrease of t_{fl} due to the increasing field strength E between the cathode and the plate is limited by the photocathode autoelectronic emission. The time t_{fl} depends also on the cathode-plate distance and cathode's area. Therefore, by selecting the photo-

element construction and electric field parameters, one can minimize t_n and get the time resolution of such radiation receiver up to values limited by the photocathode emission constant under the appropriate decrease in the load capacity at passing to strip-line photoelement constructions with low wave impedance values. The fundamentally unavoidable reason for the sluggishness of typical photoelectron multipliers is the time dispersion of the electron fly-pass between secondary emitters. But one can significantly decrease it by selection of a secondary-electron amplifier, the capacities of output circuits, and supply voltages.

A real method to increase the time resolution of optical signals in photoelectron oscillography systems is the photocurrent strobbing in PEM's near-cathode area [6]. This method eliminates the dependence of the measuring system's sluggishness on the time dispersion of the electron fly-pass through PEM's input camera between dynodes of the multiplier system and the anode load time constant by keeping, at the same time, the sensitivity to be high.

To form a stroboscopic slice with subnanosecond width out of the photocurrent, one supplies the blocking voltage for emitted electrons on a modulator near the PEM photocathode. That is, the mode of controlling the photocathode emission is created. Synchronously with an optical signal, they affect the photocurrent by a strobbing signal. At that, some part of electrons gets enough energy to overcome the potential barrier. They come to the multiplier system and the detector output. By the time shift of strobbing impulses, one gets the sequence of slices, whose envelope is a time converted optical signal, on the PEM output [6]. At the domed form of strobbing impulses of 400 V in amplitude at a 75-Ohm resistance (load) and a half-height width of 1 ns, the system's time resolution is $(2 - 4) \times 10^{-11}$ s at the threshold sensitivity of 10^{-7} W. To the disadvantages of the above-described method of strobbing in an PEM input camera, one can refer the high power consumption of the system, bad operability under optical noises and background illumination, need to select PEM by a photocathode surface resistance, and limiting the maximum length of registered optical signals. There are known also stroboscopic photooscillography systems, where the photocurrent strobbing is performed in the PEM dynode system. Here, the traveling wave mode is realized when the time of dynode system's operation in the multiplying mode is comparable with the time of the electron fly-pass between the dynodes [14]. The time resolution is several times better than that of the typical PEM switching on, but it is much less than that of systems with strobbing in the near-cathode area and is around 10^{-9} s.

By forming a stroboscopic slice from the photocurrent in a PEM by the selection of non-uniformly accelerated electrons on the time of their arrival to the dynode system [15] and by combining the modulator and dynode control (the traveling wave mode), one can create devices of photoelectron stroboscopic oscillo-

graphy for optical signals of $10^{-7} - 10^{-3}$ W in power in the wavelength range of $0.4 - 1.3 \mu\text{m}$ with a controlled time resolution of $3 \cdot 10^{-11} - 2 \cdot 10^{-9}$ s which operate under optical noises and background illumination of the optical input [16].

5. Optical stroboscopic oscilloscope OSO-1

The exploration of the generation dynamics of injection lasers was done with the help of an optical stroboscopic oscilloscope OSO-1 with time resolution of $\sim 3 \times 10^{-11}$ s. The OSO-1 structure scheme is shown in Fig. 2.

A synchronizing impulse is supplied to the sweep circuit from a pump oscillator. The time scanning sweep circuit output signal comes to the input of a cutoff voltage generator and, through the time-delay line, to the input of a strobbing impulse generator. Generators' inputs are connected to the butt PEM modulator. The sweep circuit signal is supplied through the dynodes to the controlling device. The positive blocking voltage impulse with an amplitude providing the entire photocurrent cut-off is supplied to the extrinsic wideband photocurrent modulator. Thus, the light impulse that comes to the PEM cathode simultaneously with a blocking impulse is not registered on the PEM output. By synchronously supplying a short negative impulse (a strobbing impulse) to the modulator, one can back up the initial PEM sensitivity for the time equal to the impulse time length. In this case, the photocurrent impulse is registered on the multiplier output, and it is proportional to the light intensity during the strobbing impulse.

By realizing the time shift of a strobbing impulse relative to the registered light impulse, one gets a succession of impulses on the PEM output. Their envelope is a time converted initial light impulse [18]. The converting ratio is $K_{tr} = nT_n / t_s$, where T_n is the period of strobbing impulses, n is the number of signal readings, and t_s is the signal time length. By denoting $t_s / n = \Delta t_s$, one gets $K_{tr} = T_n / \Delta t_s$.

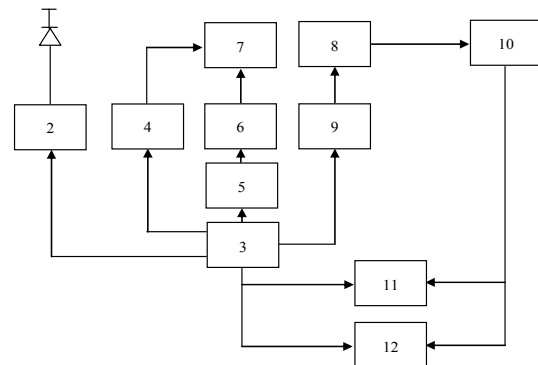


Fig. 2. Structure scheme of an oscilloscope OSO-1. 1 – light emitter, 2 – pumping generator, 3 – scanning circuit, 4 – cutoff generator, 5 – delay line, 6 – strobe impulse generator, 7 – photocurrent modulator, 8 – PEM, 9 – dynodes control scheme, 10 – processing block of an input PEM signal, 11 – electronic-beam indicator, 12 – plotter.

An automatic shift system includes a linear sawtooth voltage generator with quick raise (a quick sawtooth voltage generator) that is launched by synchronizing impulses, a slow sawtooth voltage generator, and a comparing circuit, to which the voltages from both generators are supplied. When these voltages are equal, the circuit generates impulses used to control the strobing impulse generator.

The time moment, when the voltages are equal, is automatically shifted relative to the starting point of a quick sawtooth voltage raise at every iteration of a synchronizing impulse. Every of these voltages (“quick” and “slow”) linearly changes with time (in the operating ranges), so the shift of the comparing moment is also a linear function.

The necessary number of readings is known to be determined, in accordance with the Kotelnikov theory, by the maximum reading step $\Delta t_{s\max} = 1/(2f_{\max})$ and has a value $n \geq t_s/\Delta t_{s\max}$, where f_{\max} is the highest frequency of the explored signal spectrum.

The physical time resolution of the photo-oscillographic systems with stroboscopic transformation of the PEM photocurrent is determined mainly by the ratio between control signals’ amplitudes.

Blocking impulses make a potential barrier for photoelectrons in the input camera, and strobing impulses, which exceed the blocking ones by their amplitude, accelerate the electrons in the first dynode direction. The maximum distance between electrons and a photoemitter during the acceleration is usually at most 10 % of the input camera length. As the energy transfer to electrons depends on the acceleration time length, their total energy to a great extent is determined by the relation of the photoemission moment to the start point of a strobing impulse with length t_s . For this reason and due to the selection of control impulses’ amplitudes, only electrons outgoing in the interval $\Delta t \leq t_s$ near the unblocking impulse start point can overcome the potential barrier at the further traveling in the barrier layer.

By using this method, one can eliminate the effect of the time dispersion of the electron fly-pass on the time resolution of the registration system and get the strobe slices of photoelectric signals that are by $10^2 - 10^3$ times shorter than the strobe impulse length.

OSO-1 is designed for the observation and registration of a form of repeatable optical signals in the visible and near-IR ranges of nano- and sub-nanosecond time lengths with a peak power from 10^{-7} to 10^{-3} W on the optical input; photoelectron multiplier FEM-83 or FEM-84 is used in OSO-1; the wavelength range of registered optical signals is 400–1200 nm (FEM-83) or 400–900 nm (FEM-84); the raise time of the transient characteristic is continuously adjustable in the range of $7 \times 10^{-11} - 10^{-9}$ s; scan-out range (to the whole scale): 0.1, 0.4; 1.0, 2, 5, 10, 20, 50, 100, and 200 ns; and the number of strobe points is 128, 256, 512, and 1024.

6. Method of studying

The method of studying the radiation dynamics of injection lasers is as follows: the pumping oscillator generates the excitation impulses that come to the explored source. The radiation of the source that is at the lens focus falls in the lens of an optical stroboscopic oscilloscope. On its screen, the signals of the injection laser light response are displayed. The oscilloscope has a plotter that records the results graphically. The multi-purpose high-speed oscilloscope is used to control the pumping current impulses.

This measurement method allows one to control directly the form of both pumping and radiation impulses, determine the delay time of light relative to the current impulse, and the real time length of a light impulse. Its precision was limited mainly by the time resolution of the device.

7. Analysis of self-modulation phenomena in laser diodes with saturating absorber in a resonator

Laser diodes were explored in two operation modes: at the supply of a current impulse directly to the diode and under the constant bias I_0 . Depending on the excitation modes, the threshold currents of explored lasers determined from the watt-ampere characteristics were varied in the range of 0.2 to 0.45 A.

At the impulse excitation, the spontaneous lifetime of nonequilibrium charge carriers (NCC) τ_s can be determined by the expression $t_d = \tau_s \ln \frac{I}{I - I_{th}}$, where t_d

is the radiation delay, and I and I_{th} are the pumping current and the threshold value of the pumping current, respectively. Its value was about 1-2 ns. Superposition of the current impulses and a constant bias increases greatly the injection laser’s operating speed due to the partial deletion of the radiation delay. In this case,

$$t_d = \tau_t \ln \frac{I}{I - (I_{th} - I_0)}, \quad (1)$$

where τ_t is a total NCC lifetime, I_0 is bias current.

The data on the operation speed of laser diodes were got by analyzing the dependences shown in Fig. 3. The explored diodes have exponential dependence of I_{th} on the pumping impulse width T ,

$$I_{th} = I_{cm} \left[1 - \exp\left(\frac{-T}{\tau_t}\right) \right]^{-1}, \quad (2)$$

where I_{cm} is a threshold current for a long pumping current impulse corresponding to I_{th} at the excitation by a constant current.

The study of radiation pulses at various pumping excesses over the threshold showed that the semiconductor laser radiation instability has a threshold character, i.e. it occurs only at some critical excess of the pumping over the generation threshold (Fig. 4).

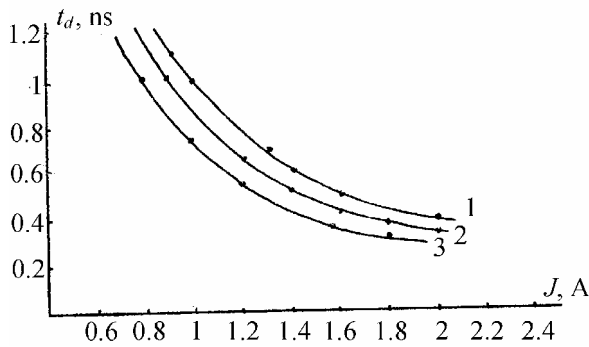


Fig. 3. Dependence of the generation delay time t_d on the pumping current I : 1 – at impulse excitation; 2 – at constant bias $I_0 = 89 \mu\text{A}$; 3 – $I_0 = 137 \mu\text{A}$. The pumping impulse width is 7 ns and the leading edge is 0.3 ns.

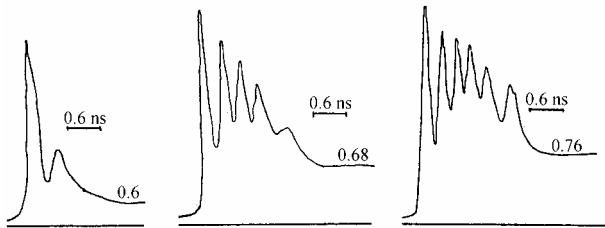


Fig. 4. Radiation impulse oscillograms of an injection DHS-laser with saturating absorber in a resonator at various pumping current values (in A). The pumping impulse width is 10 ns and the leading edge is 0.3 ns.

At studying the time dependence of the radiation intensity of an injection laser, it was found that, at the increase of the pumping, the peaks' repetition frequency that was determined by two first impulses increased (Fig. 5), that corresponds perfectly to the theoretical data.

It is worth noting that, at increasing the bias current I_0 , the pulse frequency increases firstly and then begins to decrease (Fig. 6). At low values of the bias current, one can suggest the method of a local heating of the absorbing inhomogeneity (near the surface, near the side edge of the active stripline, in “dark line” type defects, etc.). Heating increases the absorption, because a local narrowing of the band-gap occurs. The instability criterion becomes more realizable, which makes the pulses more stable. Therefore, the pulse frequency increases firstly. At a further increase of the constant bias, the laser crystal is heated, which results in a rise of the laser threshold current. Thus, the rational exceeding of the pumping over the threshold decreases, which leads to a decrease of the frequency of peaks at the bias current growth over $89 \mu\text{A}$.

The dependence $I_{th}(T)$ is often approximated by the exponential function: $I_{th}(T) = I_{th}(0) \cdot \exp(T/\theta_1)$, where θ_1 is a temperature parameter depending on the form of the semiconductor energetic spectrum in the range of working junctions. But, at high temperatures, the threshold

current density of lasers on a two-side heterostructure rises with the temperature more quickly than the exponential function. At the threshold for DHS-lasers on GaAlAs, θ_1 has values from 70 to 185 K depending on the heterolaser structure and operation conditions.

Physical reasons of the threshold increase with the temperature rise are the temperature split of degeneracy, increase of non-resonance absorption, and increase of the radiationless recombination speed with the temperature that is typical of semiconductors.

The dependence of the peaks' parameters (period and width) on the impulse pumping current amplitude and the constant bias current was also studied. At the increase of the pumping current, the period and width of peaks decrease and reach some certain limit. The width measured at the 0.5 level has, in most cases, values of 0.2 – 0.5 of the period value.

While studying the peak generation mode, it was noticed that the frequency of peaks during the pumping impulse has non-regular (instable) character. It tends to decrease at the end of a pumping impulse or the period of peaks in a succession increases (Fig. 7). It is worth also noting that, at impulse pumping of the diode, relaxation oscillations are observed.

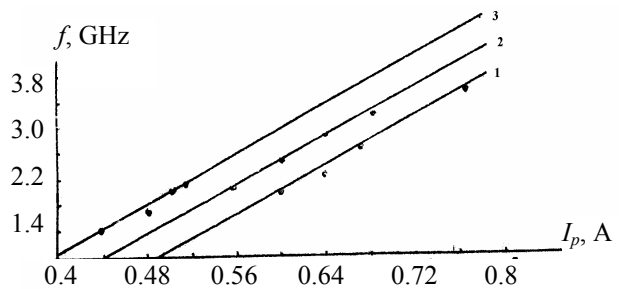


Fig. 5. Pumping current dependence of the peak frequency, determined by two first peaks, at the pumping impulse width $\tau_{pi} = 10$ ns and the leading edge $\tau_{fr} = 4$ ns (1); $\tau_{pi} = 8$ ns, $\tau_{fr} = 2$ ns (2); $\tau_{pi} = 7$ ns, $\tau_{fr} = 0.3$ ns (3).

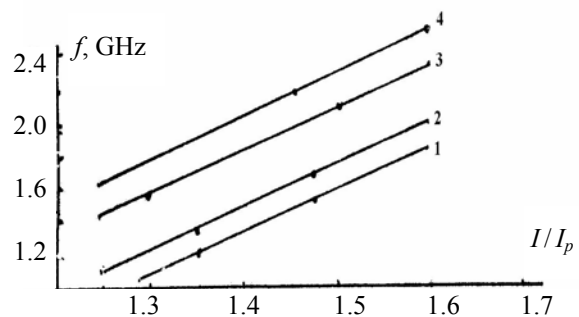


Fig. 6. Dependence of the peak frequency, determined by two first peaks, on the pumping exceeding the generation threshold at the bias current I_0 equal to 178 (1), 137 (2), 84 (3), and $89 \mu\text{A}$ (4).

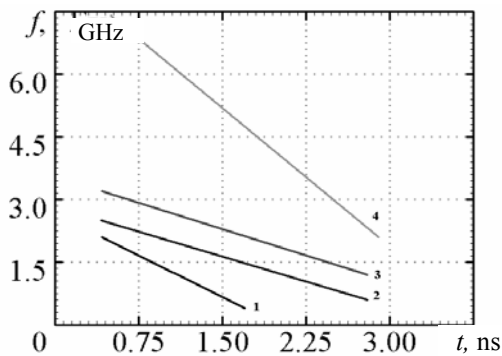


Fig. 7. Dependence of peak frequency on the time duration of a pumping impulse at pumping impulse currents of 0.29 (1), 0.3 (2), 0.31 (3), and 0.38 A (4).

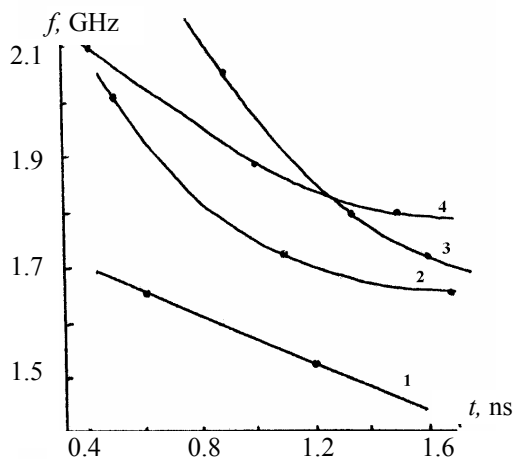


Fig. 8. Dependence of peak frequency on the time duration of a pumping impulse at pumping impulse currents of 0.44 (1), 0.48 (2), 0.54 (3), and 0.52 A (4) at $I_0 = 137 \mu\text{A}$.

At the supply of a constant bias to the p - n junction, the dependence of the peak power in a radiation impulse doesn't have relaxing character. A decrease of the frequency of peaks during the pumping impulse (Fig. 8) was also observed, which may be explained by heating the diode active area due to the radiationless recombination of electrons and holes and the absorption of spontaneous and stimulated radiation.

During the laser operation at the modulation of the resonator Q-factor in the after-threshold mode, i.e. when the pumping excess over the generation threshold is not large, somewhat near to 1.05, the pulse period is longer than the pumping impulse width. In this case, the laser generates only one light impulse – “the pulsating peak”.

In this mode, an optical radiation impulse of ~ 60 ps in width at the half-height and with the leading edge of 46 ps and the decay time of 60 ps was obtained.

8. Conclusion

We have developed a method to explore the dynamics of light generation by injection heterolasers with saturating absorber in the resonator with the use of an optical stroboscopic oscilloscope OSO-1. It allows the direct observation of auto-modulation phenomena and signal's form and also determining the radiation impulse width and the light signal delay relative to the pumping current. It has significant advantages over the indirect measurements, for example, at the use of correlation methods.

Generation of an injection heterolaser with internal modulation of the Q-factor has instable character of radiation at a certain critical pumping exceeding the generation threshold. The radiation impulse has form of a packet of peaks. There is a radiation delay between radiation impulses and current pumping impulses that decreases as the pumping current rises. This results from the need to reach the necessary redundant charge carrier concentration enough for creating the threshold population inversion in a laser.

The minority charge carrier lifetime at the before-threshold operation mode in the active area of an injection heterolaser with saturating absorber in a resonator, determined by the radiation delay, is 1 to 2 ns. The superposition of impulses and a constant current bias – prior to the pumping – greatly increases the injection heterolaser operation speed due to eliminating the radiation delay.

The peak frequency determined by two first peaks increases with the pumping current. This fact agrees perfectly with the theoretical pumping current dependence of the frequency. The peak frequency lies in the range of 1.4–4 GHz. At the supply of a current impulse to the constant current bias, the pulse frequency increases firstly and then begin to decrease, which is related to the laser crystal heating resulting in the laser threshold current rise and, consequently, in a decrease of the excess of the pumping over the threshold. This leads to a decrease in the frequency with the further rise of a constant bias current.

If the excess I_{th} isn't large, somewhat near 1.05, then the pulse iteration period is greater than the pumped impulse width. In this case, a laser generates only one light peak. We have registered the radiation impulse of 60 ps in width at the half-height with a leading edge of 46 ps and a decay time of 60 ps.

References

1. Z.I. Alferov, A.B. Zhuravlev, E.L. Portnoi, N.M. Stelmakh, Generation of picosecond impulses in injection lasers with modulated Q-factor // *Pis'ma Zhurnal Tekhnich. Fiziki* **12**(18), p. 1093-1098 (1986) (in Russian); *Fiber Optical Communication Lines. Reference Book* / Ed. by S.V. Svechnikov and L.M. Andrushko. Tekhnika, Kiev, 1988.

2. I.M. Demchuk, M.A. Ivanov, *Statistical Single-Quantum Method in Optical-Physical Experiment*. BSU, Minsk, 1981 (in Russian).
3. M.M. Butslov, B.M. Stepanov, S.D. Fanchenko, In: *Electron-Optical Converters and Their Application in Scientific Researches* / Ed. by E.K. Zavoisky. Nauka, Moscow, 1978 (in Russian).
4. G. Endrus, R.A. Lauton, Stroboscopic oscilloscope for optical signals with electrical strobbing // *Devices for Scientific Researches* **47**(3), p. 43-47 (1976).
5. J.J. Wiczer, H. Merkelo, Picosecond optical detection by high-speed sampling of photoelectrons // *Appl. Phys. Lett.* **27**(7), p. 397-399 (1975).
6. I.Z. Rutkovsky, N.N. Shavel, Stroboscopic transformation by FEM // *Experiment Devices and Technique* No. 6, p. 125-127 (1971).
7. A.F. Shilov, I.S. Manak, I.A. Kobak, On the operation of photoelectronic multipliers with photocurrent modulation in the near-cathode area // *JAS* **11**(2), p. 337-341 (1969).
8. I.A. Kobak, I.S. Manak, U.V. Popov, A.F. Shilov, Distance measurement by method of light-location with semiconductor light-emitting diode // *News of High Education Establishments. Geodesy and Aerophotography* No. 2, p. 23-28 (1974).
9. I.S. Manak, SHF-range phase detectors on photoelectronic multipliers // *Sensors and Information Converters of Systems of Measurement, Control and Manipulation. Papers of the XV Scientific-Technical Conference*, MGIEM, Moscow, 2003, p. 269-271.
10. O.M. Brekhov, V.B. Lebedev, V.B. Luzanov *et al.*, Registration of sub-picosecond impulses in radiation of neodymium and colorant laser // *Abstracts of the 10 USSR Scientific-Technical Conference "High-Speed Photography and Quick Processes Metrology", December 1981*. Institute of Optical-Physical Measurements, Moscow, 1981, p. 15.
11. I.Z. Rutkovsky, N.N. Shavel, Time resolution of stroboscopic recorder // *Experiment Devices and Technique* No. 3, p. 199-201 (1973).
12. A.F. Shilov, I.S. Manak, I.A. Kobak, Measurement system of modulation depth of the radiation in the range up to 2 GHz // *JAS* **6**(5), p. 674-675 (1967).
13. I.M. Bronshtein, S. Fraiman, *Second Electron Emission*. Nauka, Moscow, 1969 (in Russian).
14. N.A. Soboleva, A.E. Melamid, *Photoelectronic Devices*. Vysshaya Shkola, Moscow, 1974 (in Russian).
15. Inventor's certificate of the USSR No. 1382119, Intern. Cl.⁴ GOIJ 1/42, A method of forming the stroboscopic slice of the photocathode electron signal / A.S. Prohorenko, No. 4021341/24 – 21(022200).
16. I.S. Manak, S.D. Zharnikov, A.S. Prohorenko, N.M. Stelmah, Generation of picosecond impulses by injection heterolasers with saturating absorber in resonator // *Abstracts of the 3rd USSR School on Picosecond Technics. Erevan, 1988*. Institute of Optical-Physical Measurements, Moscow, 1988, p. 11-12.
17. I.S. Manak, Measurement system for the analysis of variations of generation delays in near radiation area of injection lasers, In: *Lasers. Measurements. Information.* / Ed. by V.E. Privalov. S.-Petersburg, 2004, p. 16.
18. A.S. Prohorenko, N.N. Shavel, Optical stroboscopic oscilloscope of super high time resolution for observation of time structure of repeatable optical signals // *Abstracts of the XI USSR Scientific-Technical Conference "High-Speed Photography, Photonics and Quick Processes Metrology", Moscow, 1983*. Institute of Optical-Physical Measurements, Moscow, 1983, p. 240.